Scientia Iranica B (2015) 22(2), 436–447

Sharif University of Technology
Scientia Iranica
Transactions B: Mechanical Engineering
www.scientiairanica.com

The fluid structure interaction effect on the vibration and instability of a conveyed double-walled boron nitride nanotube

A. Ghorbanpour Arani[a,b,*], Z. Khoddami Maraghi[a] and E. Haghparast[a]

a. *Department of Mechanical Engineering, Faculty of Engineering, University of Kashan, Kashan, Iran.*
b. *Institute of Nanoscience & Nanotechnology, University of Kashan, Kashan, Iran.*

Received 26 June 2013; received in revised form 3 May 2014; accepted 9 August 2014

KEYWORDS
Nonlinear vibration;
DWBNNTs;
Slip flow regime;
Knudsen number;
TB theory.

Abstract. The effect of Knudsen number (Kn) on the nonlinear vibration and instability of double-walled boron nitride nanotubes (DWBNNTs) conveying fluid has been investigated, based on Fluid Structure Interaction (FSI). The embedded DWBNNT is simulated as a Timoshenko Beam (TB), which includes rotary inertia and transverse shear deformation. The electro-mechanical governing equations are derived using the nonlocal piezoelectricity theory and discretized by a Differential Quadrature Method (DQM). Regarding the types of flow regime in FSI, including continuum, slip, transition and free molecular, the value of Knudsen number as a small size parameter is designated and utilized to modify the fluid velocity. Considering the slip condition for an internal nanotube, the effects of Knudsen number on various vibration modes, small scale, and nonlinear frequency amplitude are also taken into account for a clamped-clamped boundary condition. Results indicate that, based on the slip flow regime, the Knudsen number is an important parameter in FSI that changes the critical flow velocity and instability of nano systems and, therefore, should be considered in nanotubes conveying fluid.

1. Introduction

One of the applied branches of nano-mechanical sciences is nano-fluid structure interaction (nano-FSI), which has attracted much research into nanotechnology. Many parameters affect the mechanical behavior of a fluid, the most influential being the molecular mean free path. The mean free path is the average distance covered by a moving particle, such as a fluid molecule, between successive collisions that modify its direction or energy, or other particle properties. Whenever the length parameter of a mechanical problem is in the range of a nano-meter, it has an impacting effect on the boundary conditions of the fluid-structure interface, as well as on fluid properties, like viscosity and mass density [1]. Similarly, the Knudsen number (Kn) is a non-dimensional, small size parameter, defined as the ratio of the mean free path to the characteristic length of a geometry problem. In a micro/nano-flow field, this parameter discriminates between different flow regimes [2]:

I. $0 < \mathrm{Kn} < 10^{-2}$ for continuum flow regime;

II. $10^{-2} < \mathrm{Kn} < 10^{-1}$ for slip flow regime;

III. $10^{-1} < \mathrm{Kn} < 10$ for transition flow regime;

IV. $\mathrm{Kn} > 10$ for free molecular flow regime.

The Kn in micro/nano size FSI problems has been

*. *Corresponding author. Tel.: +98 3155 912450; Fax: +98 315 5912424*
E-mail addresses: aghorban@kashanu.ac.ir, and a_ghorbanpour@yahoo.com (A. Ghorbanpour Arani)

considered to have more than 10^{-2} value, in which the slip flow or transition flow regimes are active.

On the other hand, Boron Nitride Nano-Tubes (BNNTs) are selected in this nano-system. They show great promise due to their mechanical and thermal properties. BNNTs, apart from having high mechanical, electrical and chemical properties, prove more resistant to oxidation than carbon nanotubes (CNTs). It has, therefore, found multiple applications for BNNTs, including mechanical reinforcements and composites, batteries, fuel cell components, transistors and biosensors.

In recent years, a large amount of research work has been carried out into the buckling and vibration of nano-tubes/micro-tubes conveying fluid. Based on the TB theory, Chang and Lee [3] analyzed the effects of flow velocity on the vibration frequency and mode shape of the fluid-conveying single walled carbon nanotube (SWCNT). Their results indicate that the real component of the frequency of a higher mode is always larger than that of a lower mode for different flow velocities. Sällström and Kesson [4] worked on an exact finite element method for advanced study of the free and forced non-synchronous harmonic linear vibrations of piecewise, uniform, straight beam structures. They considered that the beam was surrounded by a Winkler-type ambient medium which conveyed a piecewise constant-speed plug flow of material along the deflected beam axis. An exact, complex-valued, non-symmetric stiffness matrix was established for a uniform beam element, based on the generalized second-order Rayleigh-Timoshenko beam theory, and the exact member stiffness matrices are also found for the Euler-Bernoulli Beam theory (EBB) and strings. Narendar and Gopalakrishnan [5] researched the effect of nonlocal scaling parameters on terahertz wave propagation in fluid filled SWCNTs. The SWCNT was modeled as a TB, including rotary inertia and transverse shear deformation, by considering the nonlocal effects, and a uniform fluid velocity of 1000 m/s was assumed. Their results showed that, for a fluid filled SWCNT, the wave number of flexural and shear waves will increase, and corresponding wave speeds will decrease, compared to an empty SWCNT. Also, the frequency decreases with an increase in the nonlocal scaling parameter, for both wave modes. They showed that the effect of fluid density and velocity have no remarkable effect on the frequencies of flexural and shear wave modes. Wang [6] presented an analytical model for predicting inner and outer layer effects on the free vibration of fluid-conveying nano-tubes, based on the nonlocal elasticity theory. They indicated that the surface effects with a positive elastic constant or positive residual surface tension tend to increase the natural frequency and critical flow velocity. Also, Lei et al. [7] and Gheshlaghi and Hasheminejad [8] investigated surface effects on the free vibration of nanotubes, based on nonlocal TB and EB local beams, respectively.

Based on the strain gradient theory, Yin et al. [9] researched the size effect on the vibration and stability of micro-scale pipes conveying fluid. They revealed that the strain gradient theory is more accurate than the modified couple stress theory. Ghorbanpour and Arani et al. [10] utilized a modified couple stress theory to study the nonlinear vibration and stability analysis of DWBNNTs conveying fluid embedded in a visco-Pasternak foundation. They concluded that the length scale parameter has an important role to play in the vibration and stability of DWBNNTs.

The electro-thermo nonlinear vibration and instability of embedded DWBNNTs conveying viscose fluid are studied, based on the nonlocal piezoelectricity theory and EBB model, by Khoddami and Maraghi et al. [11]. Their results indicate that the small scale parameter, elastic medium, temperature change and electric potential have significant effects on dimensionless natural frequency and critical fluid velocity. Furthermore, the effect of fluid viscosity on the vibration of DWBNNTs may be ignored.

The effects of the type of flow regime and Knudsen number have not been considered in any of the research mentioned above.

In the following, the work in which the Knudsen number has an important role to play in results is introduced. The effect of nano-flow on the vibration of a nano-pipe conveying fluid, using the Knudsen number (Kn) effect and EBB plug-flow beam theory, was investigated by Mirramezani and Mirdamadi [2]. They rewrote the Navier-Stokes equations, with modified versions of Kn-dependent flow velocity, and showed that, for the passage of gas through a nano-pipe with non-zero Kn, the critical flow velocities decreased considerably, as opposed to those for zero Kn. They indicated that ignoring the Kn effect on gas nano-flow may cause the non-conservative design of nano-devices. Ghorbanpour Arani and Amir [12] studied the electro-thermal vibration of two BNNTs, which are coupled by a visco-Pasternak medium using the strain gradient theory and a Euler-Bernoulli model in which one of the BNNTs is conveying fluid. In this paper, the effects of Knudsen number, aspect ratio, thermal and electric fields, velocity of conveying fluid and visco-Pasternak coefficients, on the stability of a coupled system were investigated. Mirramezani et al. [13] studied the vibration of CNT conveying fluid using four theories, including classical, nonlocal, strain gradient and strain/inertia gradient theories. They showed that the forces acting between a fluid element and a neighboring CNT wall could be implemented as action and reaction forces in opposite directions. Then,

the motion equations of CNT conveying viscose and non-viscose fluids are the same.

A new coefficient for the distribution of viscosity in terms of Kn is used by Roohi and Darbandi [14]. They presented a new formulation for variation of fluid viscosity in terms of size effects, using Information Preservation simulations (IP), and considering shear stress distribution. Rashidi et al. [15] studied the divergence-type, single-mode stability of nano-tubes conveying fluid in a slip flow regime with slip boundary conditions and Kn parameter using the simply-supported Euler-Bernoulli beam theory. In order to compensate for the size-free continuum formulation of fluid dynamics (Navier-Stokes equations) by size effects, and the effects of the molecular mean free path through Kn, they suggested a non-dimensional parameter called the Velocity Correction Factor (VCF). They concluded that Kn decreases divergence mode critical gas velocity and that this influence on critical liquid velocity can be ignored. The influence of Knudsen number on fluid viscosity for the analysis of divergence in fluid conveying nano-tubes was investigated by Kaviani and Mirdamadi [1]. They studied the effects of Knudsen number and slip boundary condition on the viscosity of nano-flow passing through a nano-tube. Since the dimensionless parameter, Kn, as a small size parameter, considerably influences the stability behavior and critical flow velocity of a nano-tube conveying gas fluid, they demonstrated that with an increase in Kn, at first, the fluid viscosity would change drastically, and, with a further increase in Kn, representing a traverse of the slip layer, the rate of these changes will decrease and become approximately uniform.

The behavior of smart materials such as BNNTs has been a topic of great interest in nano-mechanics. The present work is motivated by the use of the piezoelectricity theory to study the nonlinear vibration and instability response of DWBNNTs conveying fluid embedded in a Pasternak foundation, due to the lack of study in this area. The TB theory is used for modeling DWBNNT, which is better than the EBB, since the effects of shear deformation and rotary inertia are considered. Most importantly, in this work, the effect of Knudsen number has been considered. Since the slip or transition regime govern conveyed nanotubes, it is recommended to apply a small size parameter (Kn) to obtain more accurate results. Furthermore, the effects of slip flow regime on critical fluid velocity, dimensionless small scale and frequency amplitude are discussed in detail.

2. Fundamental equations

A schematic diagram of a fluid-conveying embedded DWBNNT modeled as a TB is shown in Figure 1 in

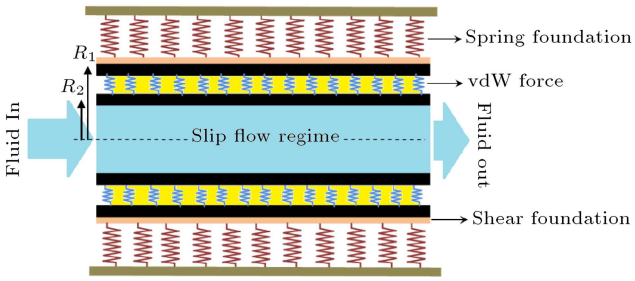

Figure 1. A DWBNNTs conveying viscous fluid embedded in an elastic medium modeled as the nonlocal Timoshenko nano-beam.

which the geometrical parameters of length, L, inner radius, R_1, outer radius, R_2, and thickness, h, are also indicated.

Using the TB theory, displacement fields are assumed as [16]:

$$\tilde{U}_i(x,z,t) = U_i(x,t) + z\psi_i(x,t),$$

$$\tilde{V}_i(x,z,t) = 0,$$

$$\tilde{W}_i(x,z,t) = W_i(x,t), \tag{1}$$

where $\tilde{U}_i$, $\tilde{V}_i$ and $\tilde{W}_i$ denote the longitudinal, circumferential and transverse displacements of the middle surface, respectively. Also, ψ_i is the rotation of the beam cross-section and t is time. It is noted that $i = 1,2$ represent the inner and outer nano-tubes. Using the above equation, the nonlinear strain-displacement von Karman relations are considered as:

$$\varepsilon_{xxi} = \frac{\partial U_i}{\partial x} + \frac{1}{2}\left(\frac{\partial W_i}{\partial x}\right)^2 + z\frac{\partial \psi_i}{\partial x}, \tag{2}$$

$$\gamma_{xzi} = \frac{\partial W_i}{\partial x} + \psi_i. \tag{3}$$

Using Eqs. (2) and (3), the total electrostatic energy of DWBNNT can be expressed as:

$$\begin{aligned} U =& \frac{1}{2}\int_0^l \left\{ N_{xi}\frac{\partial U_i}{\partial x} + M_{xi}\frac{\partial \psi_i}{\partial x} + \frac{1}{2}N_{xi}\left(\frac{\partial W_i}{\partial x}\right)^2 \right. \\ & + Q_{xi}\frac{\partial W_i}{\partial x} + Q_{xi}\psi_i \\ & + Ae_{11}\frac{\partial U_i}{\partial x}\frac{\partial \phi_i}{\partial x} + \frac{1}{2}e_{11}A_i\left(\frac{\partial W_i}{\partial x}\right)^2\frac{\partial \phi_i}{\partial x} \\ & \left. - A_i \in_{11}\left(\frac{\partial \phi_i}{\partial x}\right)^2 \right\} dx, \end{aligned} \tag{4}$$

where ϕ, $\in_{11}$ and e_{11} are the electric potential, dielectric constant and piezoelectric coefficient, respectively.

Also, N_{xi}, M_{xi} and Q_{xi} denote the resultant force, bending moment and transverse shear force, respectively, which can be defined as:

$$N_{xi} = \int_A \sigma_{xxi} dA_i,$$

$$M_{xi} = \int_A \sigma_{xxi} z dA_i,$$

$$Q_{xi} = \int_A \sigma_{xzi} dA_i. \tag{5}$$

The kinetic energy of DWBNNT can be written as follows:

$$K = \frac{\rho_t A_i}{2} \int_0^L \left[\left(\frac{\partial \tilde{U}_i}{\partial t} \right)^2 + \left(\frac{\partial \tilde{W}_i}{\partial t} \right)^2 \right] dx, \tag{6}$$

where ρ_t is the density of BNNT.

The work undertaken due to the surrounding elastic medium and vdW forces can be written as:

$$\Omega = \frac{1}{2} \int_0^L q_1 W_1 dx + \frac{1}{2} \int_0^L q_2 W_2 dx + \frac{1}{2} \int_0^L F_{\text{Elastic medium}} W_2 dx. \tag{7}$$

The second term of Eq. (7) is related to the vdW force, which can be expressed as:

$$q_1 = c(W_2 - W_1), \tag{8}$$

$$q_2 = -c \frac{R_1}{R_2} (W_2 - W_1), \tag{9}$$

where, c is the vdW interaction coefficient. The third term of Eq. (7) is related to the elastic medium. Based on the Winkler and Pasternak foundations, the effect of the surrounding elastic medium on the outer nano-tube is written as follows [17]:

$$F_{\text{Elastic medium}} = k_W W_2 - k_G \nabla^2 W_2, \tag{10}$$

where k_W and k_G are Winkler's spring modulus and Pasternak's shear modulus of elastic medium, respectively.

Figure 2 shows the velocity field, $\vec{V} = (V_x, V_z)$, for the fluid conveyed through the inner nano-tube. For the beam model, V_x and V_z are defined as [18]:

$$V_x = \frac{\partial \tilde{U}_1}{\partial t} + U_f \cos\theta, \tag{11}$$

$$V_z = \frac{\partial \tilde{W}_1}{\partial t} - U_f \sin\theta, \tag{12}$$

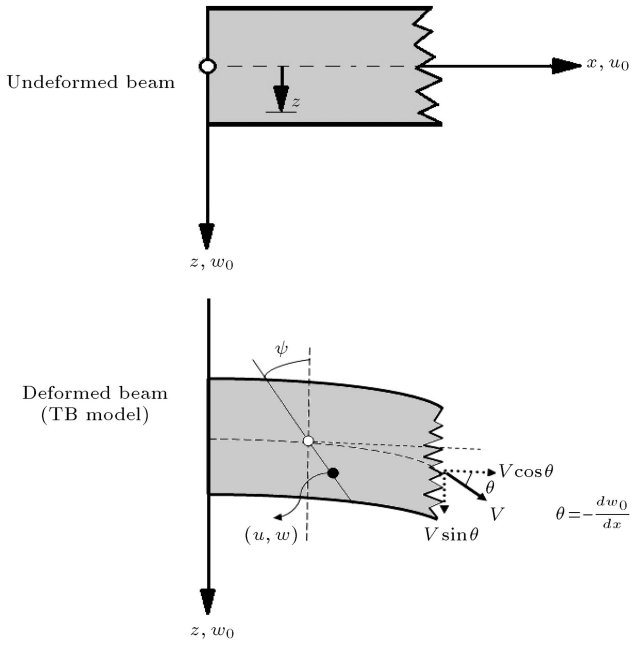

Figure 2. Deformation of a transverse normal line in Timoshenko beam model.

where U_f is the constant velocity of fluid.

According to Mirramezani et al. [13], the forces acting between a fluid element and a neighboring CNT wall could be implemented as action and reaction forces in opposite directions. Then, the forces due to viscosity, as internal forces, do not appear in the motion equations. The kinetic energy of the fluid can be written as follows:

$$K = \frac{\rho_f A_1}{2} \int_0^L \left[\left(\frac{\partial V_x}{\partial t} \right)^2 + \left(\frac{\partial V_z}{\partial t} \right)^2 \right] dx, \tag{13}$$

where ρ_f is the density of the fluid.

Flow regimes in fluid structure interaction were identified by Knudsen number. The Knudsen number is a dimensionless parameter defined as the ratio of the mean-free-path of the molecules to a characteristic length scale, which is used for identifying the various flow regimes in FSI. For micro and nano-tubes, the radius of the tube is assumed as the characteristic length scale.

According to the Knudsen number, classification of the various flow regimes is given as: Continuum flow regime ($\text{Kn} < 10^{-2}$), slip flow regime ($10^{-2} < \text{Kn} < 10^{-1}$), transition flow regime ($10^{-1} < \text{Kn} < 10$), and free molecular flow regime ($\text{Kn} > 10$) [14].

Therefore, the assumption of no-slip boundary conditions is no longer credible, and a modified model must be used.

So, $V_{\text{avg,slip}}$ is replaced by VCF $\times$ $V_{\text{avg,(no-slip)}}$ in the basic equations in which VCF is determined as follows [2]:

$$\text{VCF} \equiv \frac{V_{\text{avg,slip}}}{V_{\text{avg,(no-slip)}}} = (1+a\text{Kn})\left[1+4\left(\frac{2-\sigma_v}{\sigma_v}\right)\left(\frac{\text{Kn}}{1+\text{Kn}}\right)\right], \quad (14)$$

where σ_v is the tangential momentum accommodation coefficient. For most practical applications, σ_v is chosen to be 0.7 and a can be expressed as in the following relation:

$$a = a_0 \frac{2}{\pi}\left[\tan^{-1}\left(a_1 \text{Kn}^B\right)\right], \quad (15)$$

in which, $a_1 = 4$ and $B = 0.04$ are some experimental parameters. The coefficient, a_0, is formulated as:

$$\lim_{\text{Kn}\to\infty} a = a_0 = \frac{64}{3\pi\left(1-\frac{4}{b}\right)}, \quad (16)$$

where $b = -1$.

Figure 3 shows the changes of VCF versus Knudsen number. It is concluded from this figure, for example, that when Kn = 0.02, the value of VCF is equal to VCF = 1.1711.

Using Hamilton's principle, the variation form of the equations of motion for the DWBNNT can be written as:

$$\int_{t_1}^{t_2} [\delta K - \delta U + \delta\Omega]\, dt = 0. \quad (17)$$

Substituting Eqs. (4), (6) and (7) into Eq. (17), and using the fundamental lemma of the calculus of variation, the motion equations for viscous and non-viscous fluid-conveying embedded DWBNNTs are yielded as follows:

δU_1:

$$-\frac{N_{x1}}{\partial x} - \frac{1}{2}e_{11}A_1\frac{\partial^2\phi_1}{\partial x^2} + (m_1+m_f)\frac{\partial^2 U_1}{\partial t^2}$$

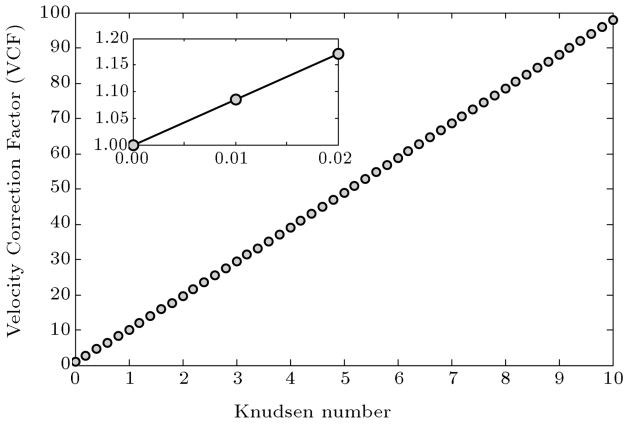

Figure 3. Variation of VCF versus Knudsen number.

$$+U_f m_f \frac{\partial^2 W_1}{\partial x\partial t}\sin\theta + m_f U_f^2\frac{\partial^2 W_1}{\partial x^2}\sin\theta = 0, \quad (18)$$

δW_1:

$$-\frac{\partial Q_{x1}}{\partial x} - \frac{\partial N_{x1}}{\partial x}\frac{\partial W_1}{\partial x} - N_{x1}\frac{\partial^2 W_1}{\partial x^2} - \frac{1}{2}A_1 e_{11}\frac{\partial^2 W_1}{\partial x^2}\frac{\partial\phi_1}{\partial x} - \frac{1}{2}A_1 e_{11}\frac{\partial W_1}{\partial x}\frac{\partial^2\phi_1}{\partial x^2} + m_f\frac{\partial^2 W_1}{\partial t^2} + m_f U_f\frac{\partial^2 U_1}{\partial x\partial t}\sin\theta - m_f U_f\frac{\partial U_1}{\partial t}\frac{\partial^2 W_1}{\partial x^2}\cos\theta + m_1\frac{\partial^2 W_1}{\partial t^2}$$

$$+2m_f U_f\frac{\partial^2 W_1}{\partial x\partial t}\cos\theta - m_f U_f\frac{\partial W_1}{\partial t}\frac{\partial^2 W_1}{\partial x^2}\sin\theta - q_1 + m_f U_f^2\frac{\partial^2 W_1}{\partial x^2}\cos\theta = 0, \quad (19)$$

$\delta\psi_1$:

$$-\frac{\partial M_{x1}}{\partial x} + Q_{x1} + (I_1+I_f)\frac{\partial^2\psi_1}{\partial t^2} = 0, \quad (20)$$

$\delta\phi_1$:

$$e_{11}A_1\frac{\partial^2 W_1}{\partial x^2} + e_{11}A_1\frac{\partial^2 W_1}{\partial x^2}\frac{\partial W_1}{\partial x} - 2\in_{11}A_1\frac{\partial^2\phi_1}{\partial x^2} = 0, \quad (21)$$

δU_2 :

$$-\frac{\partial N_{x2}}{\partial x} - \frac{1}{2}e_{11}A_1\frac{\partial^2\phi_2}{\partial x^2} + m_2\frac{\partial^2 U_1}{\partial t^2} = 0, \quad (22)$$

δW_2:

$$-\frac{\partial Q_{x2}}{\partial x} - \frac{\partial N_{x2}}{\partial x}\frac{\partial W_2}{\partial x} - N_{x2}\frac{\partial^2 W_2}{\partial x^2} - e_{11}A_2\frac{\partial^2 W_2}{\partial x^2}\frac{\partial\phi_2}{\partial x} - \frac{1}{2}e_{11}A_2\frac{\partial W_2}{\partial x}\frac{\partial^2\phi_2}{\partial x^2} + m_2\frac{\partial^2 W_2}{\partial t^2} - q_2 + K_w W_2 - K_G\nabla^2 W_2 = 0, \quad (23)$$

$\delta\psi_2$:

$$-\frac{\partial M_{x2}}{\partial x} + Q_{x2} + I_2\frac{\partial^2\psi_1}{\partial t^2} = 0, \quad (24)$$

$\delta\phi_2$:

$$e_{11}A_2\frac{\partial^2 U_2}{\partial x^2} + e_{11}A_2\frac{\partial^2 W_2}{\partial x^2}\frac{\partial W_2}{\partial x} - 2\in_{11}A_2\frac{\partial^2\phi_2}{\partial x^2} = 0. \quad (25)$$

3. Nonlocal piezoelectricity theory

There is a coupling between electrical and mechanical fields in piezoelectric materials. According to the nonlocal piezoelectricity theory [19], the constitutive equations, including stress, σ_{ij}, and strain, ε_{kl}, tensors on the mechanical side, as well as flux density, D_m, and field strength, E_k, vectors on the electrostatic side, may be combined as follows [20]:

$$(1-(e_0a)^2\nabla^2)\sigma_{ij} = c_{ijkl}\varepsilon_{kl} - e_{mij}E_m, \tag{26}$$

$$(1-(e_0a)^2\nabla^2)D_m = e_{mij}\varepsilon_{ij} + \in^S_{mk} E_k, \tag{27}$$

where c_{ijkl}, e_{mij} and $\in^S_{mk}$ are elastic compliances, the piezoelectric module and the dielectric permittivity constant, respectively. Also, e_0a denotes the small scale effect. It is also noted that the electric field, E, can be written in terms of electric potential ($E=-\nabla\phi$). According to the assumption of the TB model, Eq. (30) can be written as:

$$\sigma_{xxi} - (e_0a)^2\frac{\partial^2\sigma_{xxi}}{\partial x^2} = C_{11}\left\{\frac{\partial U_i}{\partial x} + z\frac{\partial\psi_i}{\partial x} + \frac{1}{2}\left(\frac{\partial W_i}{\partial x}\right)^2\right\} + e_{11}\frac{\partial\phi_i}{\partial x}, \tag{28}$$

$$\sigma_{xzi} - (e_0a)^2\frac{\partial^2\sigma_{xzi}}{\partial x^2} = G\left[\frac{\partial W_i}{\partial x} + \psi_i\right]. \tag{29}$$

Using Eqs. (2), (3) and (5), the resultant force, bending moment and transverse shear force can be written as:

$$N_x - (e_0a)^2\frac{\partial^2 N_x}{\partial x^2} = C_{11}A\frac{\partial U}{\partial x} + \frac{1}{2}C_{11}A\left(\frac{\partial W}{\partial x}\right)^2 + e_{11}A\frac{\partial\phi}{\partial x}, \tag{30}$$

$$M_x - (e_0a)^2\frac{\partial^2 M_x}{\partial x^2} = C_{11}I\frac{\partial\psi}{\partial x}, \tag{31}$$

$$Q_x - (e_0a)^2\frac{\partial^2 Q_x}{\partial x^2} = K_sGA\left[\frac{\partial W}{\partial x} + \psi\right], \tag{32}$$

where K_s is the shear correction factor. The dimensionless parameters for DWBNNTs can be introduced as follows:

$$\zeta = \frac{x}{L},\quad (w_i,u_i) = \frac{(W_i,U_i)}{R},\quad \eta_i = \frac{L}{R_i},\quad en = \frac{e_0a}{L},$$

$$\bar{I}_i = \frac{\rho I_i}{\rho A_i R_i^2},\quad \tau = \frac{t}{L}\sqrt{\frac{E}{\rho_t}},\quad \psi = \bar{\psi},\quad f_i = \frac{EA_f}{EA_i},$$

$$\bar{\rho} = \frac{\rho_f}{\rho_t},\quad u_f = \sqrt{\frac{\rho_f}{E}}U_f,\quad \bar{C}_i = \frac{cL^2}{EA_i},\quad \beta_i = \frac{K_{si}GA_i}{EA_i},$$

$$\bar{K}_w = \frac{k_WL^2}{EA_i},\quad \bar{G}_p = \frac{k_G}{EA_i},\quad \gamma = \frac{\in_{11}E}{e_{11}^2},\quad \bar{\phi} = \frac{\phi e_{11}}{LE}. \tag{33}$$

Substituting Eqs. (30) to (32) into Eqs. (18) to (25), one obtains the governing equations in terms of the mechanical and electrical displacements that are attached in the Appendix.

4. Solution method

Motion equations could not be solved analytically due to the existence of nonlinear terms. Hence, DQM is employed, which, in essence, approximates the partial derivative of a function, with respect to a spatial variable at a given discrete point, as a weighted linear sum of the function values at all discrete points chosen in the solution domain of the spatial variable. Let F be a function representing u_i, w_i, ψ_i and ϕ_i, with respect to variable ξ, in the following domain of $(0<\xi<L)$, having N_ξ grid points along these variables. The nth-order partial derivative of $F(\xi)$ with respect to ξ, may be expressed discretely [21] at point (ξ_i), as:

$$\frac{d^nF(\xi_i)}{d\xi^n} = \sum_{k=1}^{N_\xi} A_{ik}^{(n)}F(\xi_k) \qquad n=1,\cdots,N_\xi-1, \tag{34}$$

where $A_{ik}^{(n)}$ is the weighting coefficient associated with the nth-order partial derivative of $F(\xi)$, with respect to ξ, at the discrete point, ξ_i, whose recursive formulae can be found in [20,21]. A more superior choice for the positions of the grid points is the Chebyshev polynomial, as expressed in [21]. According to DQM, the mechanical clamped and free electrical boundary conditions at both ends, in each layer of DWBNNT, may be written as:

$$u_{i1} = w_{i1} = \phi_{i1} = 0, \qquad \sum_{m=1}^{N} C_{2m}^{(1)}w_{im} = 0, \quad \text{at} \quad \xi = 0, \tag{35}$$

$$u_{iN} = w_{iN} = \phi_{iN} = 0, \qquad \sum_{m=1}^{N} C_{N-1m}^{(1)}w_{im} = 0, \quad \text{at} \quad \xi = 1. \tag{36}$$

Applying these boundary conditions to the governing equations, which are presented in the Appendix, yields the following coupled assembled matrix equations:

$$\left([M] + [C_{NL}+C_L]\Omega + [K_{NL}+K_L]\Omega^2\right)\begin{pmatrix} d_b \\ d_d \end{pmatrix} = 0, \tag{37}$$

where d_b and d_d represent boundary and domain

points. $[M]$ is the mass matrix, and $[K]$ and $[C]$ are the stiffness and damping matrices, respectively, including both linear and nonlinear terms. For solving Eq. (37) and reducing it to the standard form of an eigenvalue problem, it is convenient to rewrite Eq. (37) as the following first order variable as [22]:

$$\left\{\dot{Z}\right\} = [A]\{Z\}, \tag{38}$$

in which state vector Z and state matrix $[A]$ are defined as:

$$Z = \begin{Bmatrix} d_d \\ \dot{d}_d \end{Bmatrix}, \tag{39}$$

and:

$$[A] = \begin{bmatrix} [0] & [I] \\ -\left[M^{-1}K\right] & -\left[M^{-1}C\right] \end{bmatrix}, \tag{40}$$

where $[0]$ and $[I]$ are the zero and unitary matrices, respectively. However, the frequencies obtained from the solution of Eq. (37) are complex due to the damping existing in the presence of the fluid flow. Hence, the results contain two parts; real and imaginary. The real part corresponds to the system damping, and the imaginary part represents the natural frequencies of the system.

5. Numerical results and discussion

In order to obtain the nonlinear frequency and critical fluid velocity for a fluid-conveying DWBNNT embedded in the Pasternak foundation, a computer program based on the DQM was written, where the effects of Knudsen number on different modes, fluid velocity and viscosity, nonlocal parameter and nonlinear frequency amplitude were investigated. We assume that the flowing liquid is water and its mass density is 1000 kg/m^3, while the properties of DWBNNTs are $\rho_t = 2300$ kg/m^3, $\frac{L}{R_2} = 10$, $R_1 = 11.43$ nm, $R_2 = 12.41$ nm [12].

Figures 4 and 5 show the imaginary and real parts of the dimensionless frequency versus dimensionless flow velocity for three values of Knudsen number. As can be observed from this figure, the critical fluid velocity of DWBNNT decreases with increasing Kn. The dimensionless critical flow velocity, without considering Kn, is $u_{f(\text{critical})} = u_{\text{avg,no-slip}} = 2.11$, while this value in slip flow regime with Kn = 0.01 is $u_{f(\text{critical})} = u_{\text{avg,slip}} = 2.24$. Hence, the small Knudsen number can enlarge the stability region of the system; as can be seen $u_{f(\text{critical})} = u_{\text{avg,slip}} = 1.98$ when Kn = 0.02. On the other hand, the Knudsen number is an effective parameter that changes results, and which should be considered to obtain more accuracy in nanotubes conveying fluid.

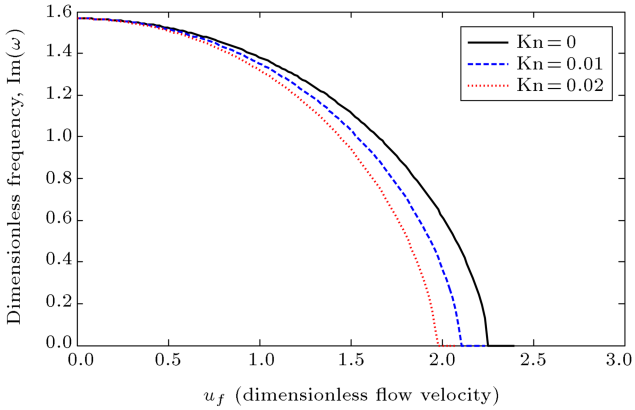

Figure 4. Imaginary part of dimensionless frequency versus dimensionless fluid velocity for various Knudsen number.

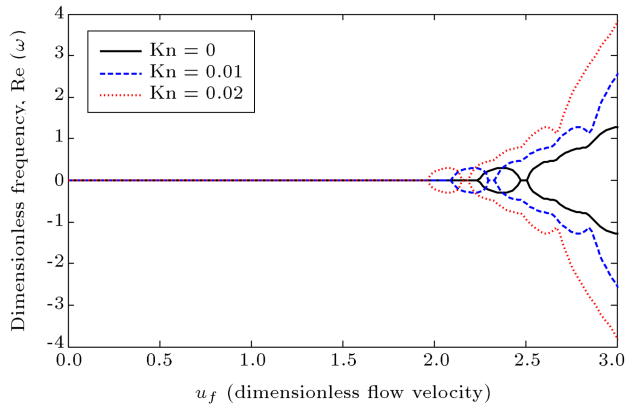

Figure 5. Real part of dimensionless frequency versus dimensionless fluid velocity for various Knudsen number.

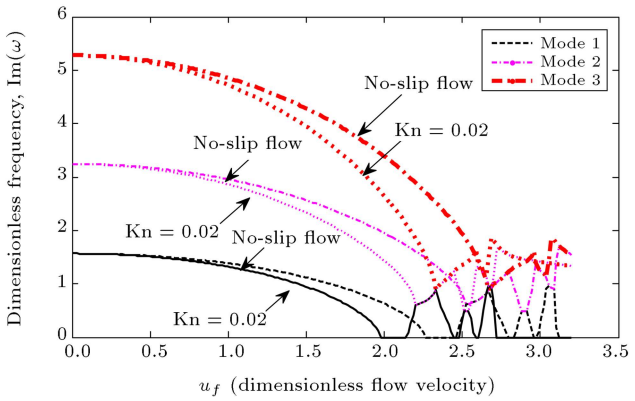

Figure 6. Imaginary part of dimensionless frequency versus dimensionless fluid velocity for the first three modes of DWBNNT.

Figures 6 and 7 have been plotted for three modes of vibration. Simultaneously, the effect of Knudsen number is investigated for every mode separately. As can be seen, the instability region shrinks when the Knudsen number appears, and this process was observed for all modes. On the other hand, the Knudsen number shows its effect on different modes.

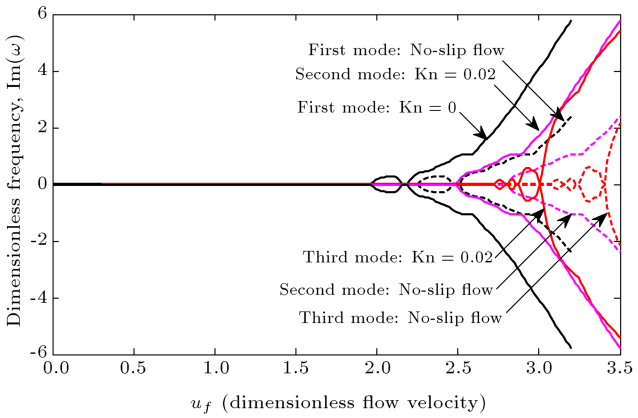

Figure 7. Real part of dimensionless frequency versus dimensionless fluid velocity for the first three modes of DWBNNT.

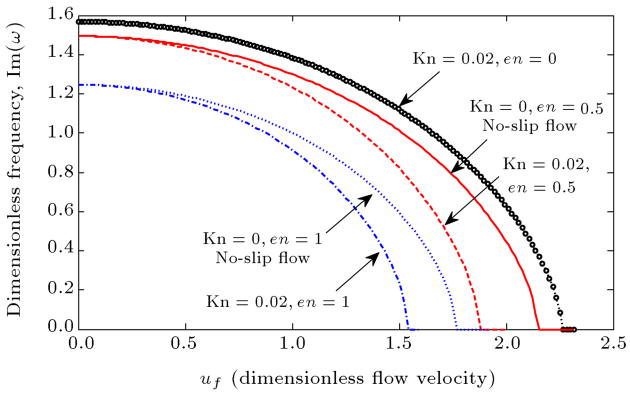

Figure 8. The effect of small scale on the imaginary part of dimensionless frequency in slip and no-slip regime.

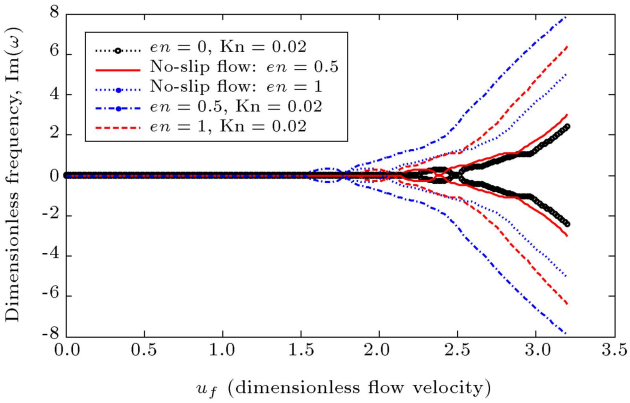

Figure 9. The effect of small scale on the real part of dimensionless frequency in slip and no-slip regime.

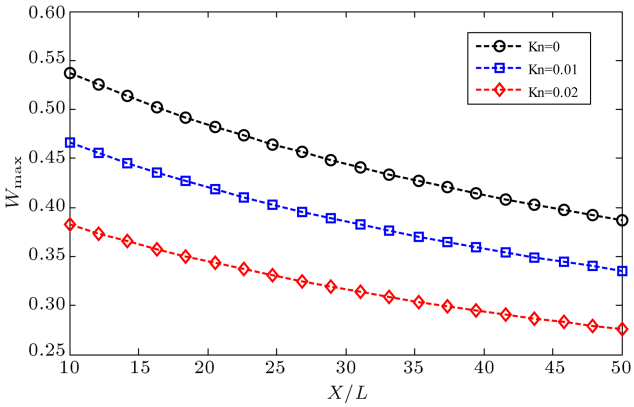

Figure 10. The effect of Knudsen number on dimensionless nonlinear frequency amplitude along BNNT in various Knudsen number.

It is noted that Im(ω) is the resonance frequency and Re(ω) is related to damping. Generally, the system is stable when the real part of the frequency remains zero, and it is unstable when the real and imaginary parts of the frequency become positive and zero, respectively. It can be seen that the Im(ω) generally decreases with increasing u_f. For zero resonance frequency, DWBNNT becomes unstable, and the corresponding fluid velocity is called the critical flow velocity. As can be seen, the critical fluid velocity corresponding to the first mode is reached at $u_f = 1.97$. Thereafter, for the slip fluid velocity within the range of $1.97 < u_f < 2.14$, the Re(ω) of the first mode is positive, at which the system becomes unstable. Afterwards, the Im(ω) of the first and second modes combine in the region of $2.2 < u_f < 2.33$. This physically implies that a single coupled-mode between the first and second modes occurs which is unstable, with flutter instability. Also, this phenomenon may be observed in different modes for higher velocities. For example, a coupled-mode between the second and third modes takes place in the range of $2.33 < u_f < 2.45$. It should also be noted that the divergence and flutter instability obtained from Figures 6 and 7 is the same as observations made by [23,24]. The real and imaginary parts of the frequency versus the flow velocity for different values of dimensionless nonlocal parameter (en) are illustrated in Figures 8 and 9, respectively. Research regarding Eringen's theory and small scale effects in slip and no-slip flow regimes is the purpose behind presenting these figures. It is noted that $en = 0$ corresponds to the classical TB model. The effect of a nonlocal parameter in both slip and no-slip regimes was investigated. As can be seen, the resonance frequency is significantly affected by en and Kn. It is observed that the Im(ω) and critical fluid velocity of DWBNNT increase with decreasing en and Kn. This is perhaps due to the fact that increasing the en decreases the interaction force between nano-tube atoms, which leads to a softer structure.

The effect of Knudsen number on nonlinear frequency amplitude along the DWBNNT is shown in Figure 10. All the figures express that when the slip flow regime governs the system, the Knudsen number, as a characterization parameter, declines the instability region. Also, in this figure, increasing Knudsen number

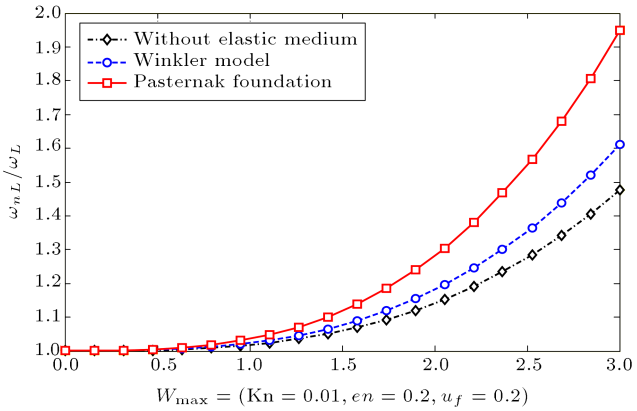

Figure 11. The effect of elastic medium on nonlinear frequency ratio versus frequency amplitude of BNNT.

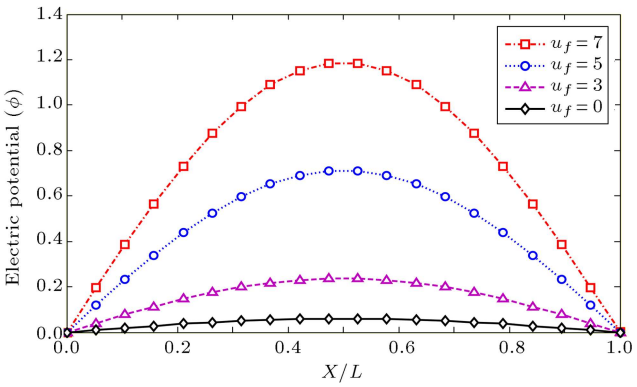

Figure 12. Distribution of electric potential along the BNNT for different values of fluid velocity.

creates a decrease in frequency amplitude, where it decreases along the DWBNNT.

In order to show the effect of nonlinear terms on the results, the nonlinear frequency ratio versus the frequency amplitude of DWBNNT is illustrated in Figure 11. This figure demonstrates that at lower frequency amplitudes of DWBNNT, the results of linear and nonlinear analyses are similar, while nonlinear terms should be considered at higher frequency amplitudes of DWBNNT. In addition, it is found from this figure that due to considering the shear effect in the Pasternak model, the stability of the system is greater than in the Winkler type.

Figure 12 depicts the distribution of electric potential (ϕ) in the DWBNNT for various fluid velocities. This figure demonstrates the excellent piezoelectric property of DWBNNTs. As can be seen, constant electrical boundary conditions at both ends of the DWBNNT are satisfied.

In Figure 12, electric potential, ϕ, is directly related to u_f. Due to coupling between mechanical and electrical fields in piezoelectric materials, the stress and deformation of DWBNNT lead to higher electric potential, as fluid velocity increases. It can be used in warning systems and sensors.

Conclusions

The effects of fluid structure interaction using Knudsen number parameters on the vibration and instability behavior of DWBNNT conveying fluid while embedded in a Pasternak foundation were investigated. The DWBNNT is modeled as a TB, and the vdW forces between two layers were considered. The nonlocal piezoelectricity theory was used to drive the motion equations according to system size (nano) and properties (Piezo). Based on the slip flow regime, the dimensionless Knudsen number was applied to the equations as a parameter that modifies fluid velocity and viscosity. Using DQM, the governing equations were solved to obtain nonlinear frequency and critical fluid velocity with clamped-clamped boundary conditions. Regarding Knudsen number, the divergence and flutter instability of DWBNNT for the first three modes of resonance frequencies are discussed in detail. The results demonstrate that decreasing the nonlocal parameter can enlarge the stability region of DWBNNT. In addition, it has been found that the vibration behavior of a system is strongly dependent on flow regime, so, increasing Knudsen number significantly decreases critical flow velocity and shrinks the instability region. Also, it is shown that the trend of the figures is in good agreement with previous research. Already, in such work, the various types of flow regime were not considered by their authors, but it is now known that they can change the results significantly. This paper indicates that the application of Knudsen number in conveyed nano-tubes is important and its consideration is recommended.

Acknowledgments

The author would like to thank the reviewers for their remarks to improve the clarity of this article. The authors are grateful to the University of Kashan for supporting this work via Grant No. 363443/2. They would also like to thank the Iranian Nanotechnology Development Committee for their financial support.

References

1. Kaviani, F. and Mirdamadi, H.R. "Influence of Knudsen number on fluid viscosity for analysis of divergence in fluid conveying nano-tubes", *Comput. Mater. Sci.*, **61**, pp. 270-277 (2012).
2. Mirramezani, M. and Mirdamadi, H.R. "The effect of Knudsen-dependent flow velocity on vibration of a nano-pipe conveying fluid", *Arch. Appl. Mech.*, **82**(7), pp. 879-890 (2012).
3. Chang, W.J. and Lee, H.L. "Free vibration of a single-walled carbon nano-tube containing a fluid flow using the Timoshenko beam model", *Phys. Lett. A.*, **373**(10), pp. 982-985 (2009).

4. Sällström, J.H. and Kesson, B. "Fluid-conveying damped Rayleigh-Timoshenko beams in transverse vibration analyzed by use of an exact finite element", *J. Fluids Struct.*, **4**(6), pp. 561-572 (1990).
5. Narendar, S. and Gopalakrishnan, S. "Terahertz wave characteristics of a single-walled carbon nano-tube containing a fluid flow using the nonlocal Timoshenko beam model", *Physica E*, **42**(5), pp. 1706-1712 (2010).
6. Wang, L. "Vibration analysis of fluid-conveying nanotubes with consideration of surface effects", *Physica E*, **43**(1), pp. 437-439 (2010).
7. Lei, X., Natsuki, T., Shi, J. and Ni, Q. "Surface effects on the vibrational frequency of double-walled carbon nano-tube using the nonlocal Timoshenko beam model", *Composites Part B*, **43**, pp. 64-69 (2012).
8. Gheshlaghi, B. and Hasheminejad, S.M. "Surface effects on nonlinear free vibration of nanobeams", *Composites Part B*, **42**(4), pp. 934-937 (2011).
9. Yin, L., Qian, Q. and Wang, L. "Strain gradient beam model for dynamics of micro-scale pipes conveying fluid", *Appl. Math. Modell.*, **35**(6), pp. 2864-2873 (2011).
10. Ghorbanpour Arani, A., Bagheri, M.R., Kolahchi, R. and Khoddami Maraghi, Z. "Nonlinear vibration and instability of fluid-conveying DWBNNT embedded in a visco-Pasternak medium using modified couple stress theory", *J. Mech. Sci. Technol.*, **27**(9), pp. 2645-2658 (2013).
11. Khoddami Maraghi, Z., Ghorbanpour Arani, A., Kolahchi, R., Amir, S. and Bagheri, M.R. "Nonlocal vibration and instability of embedded DWBNNT conveying viscose fluid", *Composites: Part B*, **45**(1), pp. 423-432 (2013).
12. Ghorbanpour Arani, A. and Amir, S. "Electro-thermal vibration of visco-elastically coupled BNNT systems conveying fluid embedded on elastic foundation via strain gradient theory", *Physica B*, **419**, pp. 1-6 (2013).
13. Mirramezani, M., Mirdamadi, H.R. and Ghayour, M. "Innovative coupled fluid-structure interaction model for carbon nano-tubes conveying fluid by considering the size effects of nano-flow and nano-structure", *Comput. Mater. Sci.*, **77**, pp.161-171(2013).
14. Roohi, E. and Darbandi, M. "Extending the Navier-Stokes solutions to transition regime in two-dimensional micro and nano channel flows using information preservation scheme", *Phys. Fluids*, **21**(8), pp. 082001-082012 (2009).
15. Rashidi, V., Mirdamadi, H.R. and Shirani, E. "A novel model for vibrations of nano-tubes conveying nanoflow", *Comput. Mater. Sci.*, **51**(1), pp. 347-352 (2012).
16. Ke, L.L., Xiang, Y., Yang, J. and Kitipornchai, S. "Nonlinear free vibration of embedded double-walled carbon nano-tubes based on nonlocal Timoshenko beam theory", *Comput. Mat. Sci.*, **47**(2), pp. 409-417 (2009).
17. Mohammadimehr, M., Saidi, A.R., Ghorbanpour Arani, A., Arefmanesh, A. and Han, Q. "Torsional buckling of a DWCNT embedded on Winkler and Pasternak foundations using nonlocal theory", *J. Mech. Sci. Technol.*, **24**(6), pp. 1289-1299 (2010).
18. Kuang, Y.D., He, X.Q., Chen, C.Y. and Li, G.Q. "Analysis of nonlinear vibrations of double-walled carbon nano-tubes conveying fluid", *Comput. Mat. Sci.*, **45**(4), pp. 875-880 (2009).
19. Eringen, A.C. "On differential equations of nonlocal elasticity and solutions of screw dislocation and surface waves", *J. Appl. Phys.*, **54**(9), pp. 4703-4710 (1983).
20. Ghorbanpour Arani, A., Kolahchi, R. and Mosallaie Barzoki, A.A. "Effect of material inhomogeneity on electro-thermo-mechanical behaviors of functionally graded piezoelectric rotating cylinder", *Appl. Math. Model*, **35**(6), pp. 2771-2789 (2011).
21. Karami, G. and Malekzadeh, P. "A new differential quadrature methodology for beam analysis and the associated differential quadrature element method", *Comput. Methods Appl. Mech. Eng.*, **191**(32), pp. 3509-3526 (2002).
22. Ke, L.L. and Wang, Y.S. "Flow-induced vibration and instability of embedded double-walled carbon nano-tubes based on a modified couple stress theory", *Physica E*, **43**(5), pp. 1031-1039 (2011).
23. Ghavanloo, E., Daneshmand, F. and Rafiei, M. "Vibration and instability analysis of carbon nano-tubes conveying fluid and resting on a linear viscoelastic Winkler foundation", *Physica E*, **42**(9), pp. 2218-2224 (2010).
24. Wang, L., Ni, Q., Li, M. and Qian, Q. "The thermal effect on vibration and instability of carbon nano-tubes conveying fluid", *Physica E*, **40**(10), pp. 3179- 3182 (2008).

Appendix

δu_1 :

$$-\frac{1}{1-\upsilon^2}\frac{\partial^2 u_1}{\partial\xi^2}-\frac{1}{1-\upsilon^2}\frac{1}{\eta_1}\frac{\partial^2 w_1}{\partial\xi^2}\frac{\partial w_1}{\partial\xi}-\frac{3}{2}\eta_1\frac{\partial^2\bar{\phi}_1}{\partial\xi^2}$$

$$+\frac{1}{2}e_n^2\eta_1\frac{\partial^4\bar{\phi}_1}{\partial\xi^4}+(1+\bar{\rho}f_1)\frac{\partial^2 u_1}{\partial\tau^2}$$

$$-e_n^2(1+\bar{\rho}f_1)\frac{\partial^4 u_1}{\partial\xi^2\partial\tau^2}-\sqrt{\bar{\rho}}f_1u_f\frac{1}{\eta_1}\frac{\partial^2 w_1}{\partial\xi\partial\tau}\frac{\partial w_1}{\partial\xi}$$

$$+e_n^2\sqrt{\bar{\rho}}f_1u_f\frac{1}{\eta_1}\frac{\partial^4 w_1}{\partial\xi^3\partial\tau}\frac{\partial w_1}{\partial\xi}$$

$$+e_n^2\sqrt{\bar{\rho}}f_1u_f\frac{1}{\eta_1}\frac{\partial^2 w_1}{\partial\xi\partial\tau}\frac{\partial^3 w_1}{\partial\xi^3}$$

$$-e_n^2\sqrt{\bar{\rho}}f_1u_f\left(\frac{1}{\eta_1}\right)^3\frac{\partial^2 w_1}{\partial\xi\partial\tau}\left(\frac{\partial^2 w_1}{\partial\xi^2}\right)^2\frac{\partial w_1}{\partial\xi}$$

$$+2e_n^2\sqrt{\bar{\rho}}f_1u_f\frac{1}{\eta_1}\frac{\partial^3w_1}{\partial\xi^2\partial\tau}\frac{\partial^2w_1}{\partial\xi^2}-f_1u_f^2\frac{1}{\eta_1}\frac{\partial^2w_1}{\partial\xi^2}\frac{\partial w_1}{\partial\xi}$$
$$+e_n^2f_1u_f^2\frac{\partial^4w_1}{\partial\xi^4}\frac{\partial w_1}{\partial\xi}+3e_n^2f_1u_f^2\frac{1}{\eta_1}\frac{\partial^2w_1}{\partial\xi^2}\frac{\partial^3w_1}{\partial\xi^3}$$
$$-e_n^2f_1u_f^2\left(\frac{1}{\eta_1}\right)^3\left(\frac{\partial^2w_1}{\partial\xi^2}\right)^3\frac{\partial w_1}{\partial\xi}=0. \quad (A.1)$$

δW_1:

$$+e_n^2\sqrt{\bar{\rho}}f_1u_f\left(\frac{1}{\eta_1}\right)^2\frac{\partial^4w_1}{\partial\zeta^4}\frac{\partial w_1}{\partial\zeta}\frac{\partial w_1}{\partial\tau}$$
$$+3e_n^2\sqrt{\bar{\rho}}f_1u_f\left(\frac{1}{\eta_1}\right)^2\frac{\partial^3w_1}{\partial\zeta^3}\frac{\partial^2w_1}{\partial\zeta^2}\frac{\partial w_1}{\partial\tau}$$
$$-e_n^2\sqrt{\bar{\rho}}f_1u_f\left(\frac{1}{\eta_1}\right)^4\left(\frac{\partial^2w_1}{\partial\zeta^2}\right)^3\frac{\partial w_1}{\partial\tau}\frac{\partial w_1}{\partial\zeta}$$
$$+2e_n^2\sqrt{\bar{\rho}}f_1u_f\left(\frac{1}{\eta_1}\right)^2\left(\frac{\partial^2w_1}{\partial\zeta^2}\right)^2\frac{\partial^2w_1}{\partial\zeta\partial\tau}$$
$$-\sqrt{\bar{\rho}}f_1u_f\frac{1}{\eta_1}\frac{\partial^2w_1}{\partial\zeta^2}\frac{\partial u_1}{\partial\tau}+e_n^2\sqrt{\bar{\rho}}f_1u_f\frac{1}{\eta_1}\frac{\partial^4w_1}{\partial\zeta^4}\frac{\partial u_1}{\partial\tau}$$
$$+3e_n^2\sqrt{\bar{\rho}}f_1u_f\frac{1}{\eta_1}\frac{\partial^3w_1}{\partial\zeta^3}\frac{\partial^2u_1}{\partial\zeta\partial\tau}$$
$$+3e_n^2\sqrt{\bar{\rho}}f_1u_f\frac{1}{\eta_1}\frac{\partial^2w_1}{\partial\zeta^2}\frac{\partial^3u_1}{\partial\zeta^2\partial\tau}$$
$$-3e_n^2\sqrt{\bar{\rho}}f_1u_f\left(\frac{1}{\eta_1}\right)^3$$
$$\frac{\partial^3w_1}{\partial\zeta^3}\frac{\partial^2w_1}{\partial\zeta^2}\frac{\partial w_1}{\partial\zeta}\frac{\partial u_1}{\partial\tau}$$
$$-3e_n^2\sqrt{\bar{\rho}}f_1u_f\left(\frac{1}{\eta_1}\right)^3\left(\frac{\partial^2w_1}{\partial\zeta^2}\right)^2\frac{\partial w_1}{\partial\zeta}\frac{\partial^2u_1}{\partial\zeta\partial\tau}$$
$$-e_n^2\sqrt{\bar{\rho}}f_1u_f\left(\frac{1}{\eta_1}\right)^3\left(\frac{\partial^2w_1}{\partial\zeta^2}\right)^3\frac{\partial u_1}{\partial\tau}$$
$$-\sqrt{\bar{\rho}}f_1u_f\frac{1}{\eta_1}\frac{\partial^2u_1}{\partial\zeta\partial\tau}\frac{\partial w_1}{\partial\zeta}+e_n^2\sqrt{\bar{\rho}}f_1u_f\frac{1}{\eta_1}\frac{\partial^4u_1}{\partial\zeta^3\partial\tau}\frac{\partial w_1}{\partial\zeta}$$
$$-\bar{\rho}f_1\bar{I}_f\left(\frac{1}{\eta_1}\right)^2\frac{\partial^4w_1}{\partial\zeta^2\partial\tau^2}+e_n^2\bar{\rho}f_1\bar{I}_f\left(\frac{1}{\eta_1}\right)^2\frac{\partial^6w_1}{\partial\zeta^4\partial\tau^2}$$
$$+f_1u_f^2\frac{\partial^2w_1}{\partial\zeta^2}-e_n^2f_1u_f^2\frac{\partial^4w_1}{\partial\zeta^4}-\bar{C}_1w_2+\bar{C}_1w_1$$
$$+e_n^2\bar{C}_1\frac{\partial^2w_2}{\partial\zeta^2}-e_n^2\bar{C}_1\frac{\partial^2w_1}{\partial\zeta^2}=0. \quad (A.2)$$

$\delta\psi_1$:

$$-\frac{\bar{I}_1}{1-\upsilon^2}\left(\frac{1}{\eta_1}\right)^2\frac{\partial^2\bar{\psi}_1}{\partial\zeta^2}+\beta_1\frac{1}{\eta_1}\frac{\partial w_1}{\partial\zeta}+\beta_1\bar{\psi}_1$$
$$+\left(\bar{I}_1+\bar{\rho}_f\bar{I}_f\right)\left(\frac{1}{\eta_1}\right)^2\frac{\partial^2\bar{\psi}_1}{\partial\tau^2}$$
$$+e_n^2\left(\bar{I}_1+\bar{\rho}_f\bar{I}_f\right)\left(\frac{1}{\eta_1}\right)^2\frac{\partial^4\bar{\psi}_1}{\partial\zeta^2\partial\tau^2}=0. \quad (A.3)$$

$\delta\phi_1$:

$$\frac{\partial^2u_1}{\partial\zeta^2}-e_n^2\frac{\partial^4u_1}{\partial\zeta^4}+\frac{1}{\eta_1}\frac{\partial^2w_1}{\partial\zeta^2}\frac{\partial w_1}{\partial\zeta}$$
$$-e_n^2\frac{1}{\eta_1}\left\{3\frac{\partial^3w_1}{\partial\zeta^3}\frac{\partial^2w_1}{\partial\zeta^2}+\frac{\partial w_1}{\partial\zeta}\frac{\partial^4w_1}{\partial\zeta^4}\right\}$$
$$-2\eta_1\gamma\frac{\partial^2\phi_1}{\partial\zeta^2}+2e_n^2\eta_1\gamma\frac{\partial^4\phi_1}{\partial\zeta^4}=0. \quad (A.4)$$

δU_2:

$$-\frac{1}{1-\upsilon^2}\frac{\partial^2u_2}{\partial\zeta^2}-\frac{1}{\eta_2}\frac{1}{1-\upsilon^2}\frac{\partial^2w_2}{\partial\zeta^2}\frac{\partial w_2}{\partial\zeta}$$
$$+\frac{1}{2}e_n^2\eta_2\frac{\partial^4\bar{\phi}_2}{\partial\zeta^4}+\frac{\partial^2u_2}{\partial\tau^2}-e_n^2\frac{\partial^4u_2}{\partial\zeta^2\partial\tau^2}-\frac{3}{2}\eta_2\frac{\partial^2\bar{\phi}_2}{\partial\zeta^2}=0. \quad (A.5)$$

δW_2:

$$-\beta_2\frac{\partial^2w_1}{\partial\zeta^2}-\eta_2\beta_2\frac{\partial\bar{\psi}_2}{\partial\xi}-\frac{1}{\eta_2}\frac{\partial^2u_2}{\partial\tau^2}\frac{\partial w_2}{\partial\zeta}$$
$$+e_n^2\frac{1}{\eta_2}\left\{\frac{\partial^4u_2}{\partial\zeta^2\partial\tau^2}+2\frac{\partial^3u_2}{\partial\zeta\partial\tau^2}\frac{\partial^2w_2}{\partial\zeta^2}+\frac{\partial^2u_2}{\partial\tau^2}\frac{\partial^3w_2}{\partial\zeta^3}\right\}$$
$$-\frac{1}{1-\upsilon^2}\frac{1}{\eta_2}\frac{\partial u_2}{\partial\zeta}\frac{\partial^2w_2}{\partial\zeta^2}$$
$$+e_n^2\frac{1}{1-\upsilon^2}\frac{1}{\eta_2}\left\{\frac{\partial^3u_2}{\partial\zeta^3}\frac{\partial^2w_2}{\partial\zeta^2}+2\frac{\partial^2u_2}{\partial\zeta^2}\frac{\partial^3w_2}{\partial\zeta^3}\right.$$
$$\left.+\frac{\partial u_2}{\partial\zeta}\frac{\partial^4w_2}{\partial\zeta^4}\right\}-\frac{1}{2}\frac{1}{1-\upsilon^2}\left(\frac{1}{\eta_2}\right)^2\left(\frac{\partial w_2}{\partial\zeta}\right)^2\frac{\partial^2w_2}{\partial\zeta^2}$$
$$+e_n^2\left(\frac{1}{\eta_2}\right)^2\left\{3\frac{\partial^3w_2}{\partial\zeta^3}\frac{\partial^2w_2}{\partial\zeta^2}\frac{\partial w_2}{\partial\zeta}+\left(\frac{\partial^2w_2}{\partial\zeta^2}\right)^3\right.$$
$$\left.+\frac{1}{2}\left(\frac{\partial w_2}{\partial\zeta}\right)^2\frac{\partial^4w_2}{\partial\zeta^4}\right\}+e_n^2\frac{\partial^3\bar{\phi}_2}{\partial\zeta^3}\frac{\partial^2w_2}{\partial\zeta^2}+\frac{\partial^2w_2}{\partial\tau^2}$$
$$-e_n^2\frac{\partial^4w_2}{\partial\zeta^2\partial\tau^2}+\bar{K}_ww_2-e_n^2\bar{K}_w\frac{\partial^2w_2}{\partial\zeta^2}-\bar{G}_p\frac{\partial^2w_2}{\partial\zeta^2}$$

$$+ e_n^2 \bar{G}_p \frac{\partial^4 w_2}{\partial \zeta^4} - \bar{C}_2 w_1 + e_n^2 \bar{C}_2 \frac{\partial^2 w_1}{\partial \zeta^2} + \bar{C}_2 w_2$$

$$- e_n^2 \bar{C}_2 \frac{\partial^2 w_2}{\partial \zeta^2} - 2\frac{\partial^2 w_2}{\partial \zeta^2}\frac{\partial \bar{\phi}_2}{\partial \zeta} + 2e_n^2 \left\{ \frac{\partial^4 w_2}{\partial \zeta^4}\frac{\partial \bar{\phi}_2}{\partial \zeta} \right.$$

$$\left. + 2\frac{\partial^3 w_2}{\partial \zeta^3}\frac{\partial^2 \bar{\phi}_2}{\partial \zeta^2} + \frac{\partial^2 w_2}{\partial \zeta^2}\frac{\partial^3 \bar{\phi}_2}{\partial \zeta^3} \right\} = 0. \quad (A.6)$$

$\delta\psi_2$:

$$-\frac{\bar{I}_2}{1-v^2}\left(\frac{1}{\eta_2}\right)^2 \frac{\partial^2 \bar{\psi}_2}{\partial \zeta^2} + \beta_2 \frac{1}{\eta_2}\frac{\partial w_2}{\partial \zeta} + \beta_2 \bar{\psi}_2$$

$$+ \left(\bar{I}_2 + \bar{\rho}_f \bar{I}_f\right)\left(\frac{1}{\eta_2}\right)^2 \frac{\partial^2 \bar{\psi}_2}{\partial \tau^2}$$

$$+ e_n^2 \left(\bar{I}_2 + \bar{\rho}_f \bar{I}_f\right)\left(\frac{1}{\eta_2}\right)^2 \frac{\partial^4 \bar{\psi}_2}{\partial \zeta^2 \partial \tau^2} = 0. \quad (A.7)$$

$\delta\phi_2$:

$$\frac{\partial^2 u_2}{\partial \zeta^2} - e_n^2 \frac{\partial^4 u_2}{\partial \zeta^4} + \frac{1}{\eta_2}\frac{\partial^2 w_2}{\partial \zeta^2}\frac{\partial w_2}{\partial \zeta}$$

$$- e_n^2 \frac{1}{\eta_2}\left\{ 3\frac{\partial^3 w_2}{\partial \zeta^3}\frac{\partial^2 w_2}{\partial \zeta^2} + \frac{\partial w_2}{\partial \zeta}\frac{\partial^4 w_2}{\partial \zeta^4} \right\}$$

$$- 2\eta_2 \gamma \frac{\partial^2 \bar{\phi}_2}{\partial \zeta^2} + 2e_n^2 \eta_2 \gamma \frac{\partial^4 \bar{\phi}_2}{\partial \zeta^4} = 0. \quad (A.8)$$

Biographies

Ali Ghorbanpour Arani received his BS degree from Sharif University of Technology, Tehran, Iran, in 1988, his MS degree from Amirkabir University of Technology, Tehran, Iran, in 1991, and his PhD degree from Esfahan University of Technology, Esfahan, Iran, in 2001. Dr. Ali Ghorbanpour Arani is currently Professor in the Mechanical Engineering Faculty of the University of Kashan, Kashan, Iran. He has authored more than 126 refereed journal papers and 10 books. His current research interests include stress analyses, stability and vibration of nano-tubes, nano-composites and functionally graded materials.

Zahra Khoddami Maraghi received her BS and MS degrees in 2008 and 2011, respectively, from the University of Kashan, Iran, where she is currently a PhD student. She has authored 9 refereed journal papers. Her research interests include bio-mechanics, nano-mechanics, and the vibration and instability of smart materials.

Elham Haghparast received her BS and MS degrees in 2011 and 2013, respectively, from the University of Kashan, Iran, where she is currently a PhD student. Her research interests include bio-mechanics and the vibration and instability of nano-composite materials.